Acta Crystallographica Section A
Foundations of Crystallography
ISSN 0108-7673

Received 21 March 2011
Accepted 15 June 2011

Anisotropy of extinction: extrapolation to the kinematical limit by γ-ray diffraction

W. Jauch* and M. Reehuis

Helmholtz-Zentrum Berlin für Materialien und Energie, Hahn-Meitner-Platz 1, D-14109 Berlin, Germany. Correspondence e-mail: jauch@helmholtz-berlin.de

A direct experimental approach to the problem of anisotropic extinction is presented. Structure-factor measurements from a vanadium and a niobium crystal, performed with four γ-ray wavelengths in the range 0.02–0.06 Å, substantiate the adequacy of Zachariasen's theory [*Acta Cryst.* (1967), **23**, 558–564] in high-energy diffraction, which provides a theoretical basis for the extrapolation to zero extinction values. Fitting of the theoretical curve to the observed points, placed on a common scale, allows determination of the kinematical structure-factor value without the need for a particular model of anisotropy in the mosaic structure.

1. Introduction

The work presented here complements and expands earlier results (Palmer & Jauch, 1995; Jauch & Palmer, 2002), dealing with the experimental accessibility of extinction-free structure factors. Our interest in this problem was rekindled by charge-density studies of vanadium and niobium. In the course of data collection, it became clear that serious anisotropic extinction effects were present in both crystals (Jauch & Reehuis, 2011). Overcoming the anisotropy problem turned out to be crucial for an unequivocal determination of the intensities of the two innermost reflections 110 and 200, which are extremely sensitive to small changes in the valence charge distribution.

A highly anisotropic mosaic block orientation was also found in a recent γ-ray study of cobalt (Jauch & Reehuis, 2009). Misorientation about the hexagonal growth axis of the crystal was much larger than that perpendicular to it. The ensuing anisotropy in secondary extinction could be fairly well described by the Thornley & Nelmes (1974) form for the angular distribution, with adjusted mosaicities close to the directly observed ones. The anisotropy problem was greatly simplified by the fact that the second-rank mosaic spread tensor had the point symmetry of the crystal, so that the number of independent elements was reduced from six to two. In general, the extinction tensor does not have to conform to the crystal symmetry, and anisotropic extinction corrections should be considered with great care since they may correlate with other anisotropy parameters, eventually leading to false conclusions. It is this concern that prompted the present approach of evading an anisotropic extinction model.

Extinction-free structure-factor values can be attained by a series of measurements involving a certain range of wavelengths. A prerequisite of such an inquiry is an adequate theoretical description of the wavelength dependence of extinction. On the experimental side, the wavelength range must be large enough and close to zero wavelength to lead to reliable estimates of the kinematical values. The last point may be illustrated for the case of a straight-line fit $y = a + bx$, where the correlation between the uncertainties of the slope b and the intercept a depends on the origin of the x coordinate. An origin well outside the data range will lead to a strong correlation, which is much reduced if the data are close to the origin.

2. Experimental

Vanadium and niobium have body-centred cubic structures with lattice constants a(V) = 3.0240 Å and a(Nb) = 3.3004 Å. The sizes of the V and Nb single crystals were 2.57 × 2.56 × 2.55 mm and 2.71 × 2.57 × 2.43 mm, respectively. The use of reasonably large samples in combination with penetrating γ-radiation avoids errors arising from inhomogeneity of the state of crystal perfection. When small specimens are employed at short-wavelength synchrotron beams, the presence of a rather perfect interior core surrounded by a less perfect surface will substantially affect the reflection intensities, and estimates of the actual amount of extinction are liable to be in error. For example, in a 100 keV synchrotron X-ray study of Cu_2O, Lippmann & Schneider (2000) found a core-to-surface volume ratio close to one.

The diffraction experiments were performed on the γ-ray diffractometer at the Helmholtz-Zentrum Berlin, which is equipped with a ^{192}Ir source ($T_{1/2}$ = 73.83 d). Rocking curves were recorded in double-crystal configuration, with a perfect Si crystal (angular resolution 1.5 arcsec) before the specimen. For vanadium, the profiles were composed of several close constituents that could not be fully resolved, but an angular FWHM of around 30 arcsec was perceptible. For niobium, a moderate anisotropy was observed with an FWHM variation between 2.2 and 2.7 arcmin.

Extinction anisotropy is most pronounced for the strongest reflections. In the γ-ray data sets of V and Nb (complete to

Table 1
Absolute values of F^2 and associated standard deviations at the four different wavelengths for vanadium.

FWHM and $F^2(\lambda = 0)$ are the parameters obtained by fitting Zachariasen's model to the observations. The calculated values, F_c^2, are derived from multipole model refinements of an extended data set.

	hkl							
	110	101	01$\bar{1}$	200	020	211	121	112
F^2 (0.0205 Å)				589 (6)	572 (6)	437 (5)	431 (5)	428 (5)
F^2 (0.0265 Å)	844 (3)	802 (3)	830 (3)	587 (2)	566 (2)	429 (2)	425 (2)	424 (2)
F^2 (0.0392 Å)	724 (1)	665 (1)	705 (1)	525 (1)	493 (1)	397 (1)	391(1)	385 (1)
F^2 (0.0602 Å)	578 (3)	518 (3)	559 (3)	443 (2)	399 (2)	349 (2)	339(2)	334 (2)
FWHM (arcsec)	27.4 (6)	18.4 (4)	23.0 (5)	20.8 (5)	14.6 (3)	18.8 (8)	16.8 (6)	16.1 (6)
$F^2(\lambda = 0)$	986 (7)	989 (9)	985 (8)	641 (3)	643 (4)	456 (3)	455 (3)	454 (3)
F_c^2	989	989	989	640	640	453	453	453

Table 2
Absolute values of F^2 and associated standard deviations at the four different wavelengths for niobium.

FWHM and $F^2(\lambda = 0)$ are the parameters obtained by fitting Zachariasen's model to the observations. The calculated values, F_c^2, are derived from multipole model refinements of an extended data set.

	hkl					
	110	01$\bar{1}$	200	020	002	211
F^2 (0.0205 Å)			2782 (29)	2750 (27)	2770 (23)	2197 (23)
F^2 (0.0265 Å)	3432 (14)	3583 (14)	2750 (11)	2719 (11)	2761 (12)	2187 (12)
F^2 (0.0392 Å)	3015 (8)	3366 (8)	2585 (7)	2540 (7)	2643 (6)	2074 (6)
F^2 (0.0602 Å)	2487 (11)	2920 (10)	2357 (10)	2273 (10)	2494 (9)	1894 (9)
FWHM (arcmin)	1.63 (4)	3.05 (9)	2.25 (9)	1.90 (7)	3.77 (8)	1.68 (9)
$F^2(\lambda = 0)$	3848 (25)	3857 (19)	2861 (13)	2859 (14)	2817 (12)	2263 (12)
F_c^2	3882	3882	2798	2798	2798	2198

$\sin\theta/\lambda = 1.9$ Å^{-1}) the first two reflections, 110 and 200, appeared to be affected by anisotropic extinction with marked intensity differences between symmetry equivalents. Measurements at different azimuthal settings ψ around the scattering vector rejected multiple diffraction as a possible cause. The very small number of data with detectable anisotropy precludes a refinement of six independent tensor components.

Four γ-lines of wavelength 0.0205, 0.0265, 0.0392 and 0.0602 Å were used to determine the three lowest-order reflections, including some symmetry equivalents. Each wavelength was selected by means of a single-channel analyser. Owing to a reduction in incident flux and crystal reflectivity, intensities at $\lambda = 0.0205$ Å are relatively weak and consequently less precise. The linear absorption coefficients μ were taken from Hubell & Seltzer (1995), and absorption corrections were performed by the analytical method implemented in *Xtal* (Hall *et al.*, 1995). For inter-wavelength scaling (incoming flux, detector efficiency), a few reflections of intermediate intensity were measured to 1% counting statistical precision or better. Their absolute values are known from the accurate structural parameters, with remaining weak extinction being taken into account. The final absolute scale was obtained by combining the extrapolated data with the extended data sets at $\lambda = 0$ 0.0392 Å. The final scale in F^2 differed from the preliminary one by 2% and 1.3% for V and Nb, respectively.

Absolute values of F^2 at the four different photon energies are reported in Tables 1 and 2. At the shortest wavelength, the innermost reflections {110} suffered from a large background, arising from the very small Bragg angles down to $\theta = 0.25^\circ$, and eluded a determination of adequate accuracy. The {200} intensities for V appear to be too small by about 2% at $\lambda = 0.0205$ Å. The magnitude of intensity diminution indicates the possibility that multiple diffraction has been operative for this orientation. Because of a lack of time, the low-order reflections were checked for multiple diffraction only with the most intense γ-line ($\lambda = 0.0392$ Å).

3. Results

According to Zachariasen (1967), the extinction coefficient, defined by $y = I_{\rm obs}/I_{\rm kin}$ as the ratio of the observed integrated intensity to its kinematical value, has the simple form $y = (1 + 2x)^{-1/2}$ where $x = g\,\overline{T_\mu}\,\lambda^2(F/V)^2 d$ for small Bragg angles as in γ-ray diffraction ($g = 0.6643$/FWHM [rad] for a Gaussian mosaic distribution, $\overline{T_\mu}$ = absorption-weighted mean path length of the diffracted beam, F = kinematical structure factor in units of scattering length, V = unit-cell volume, d = interplanar distance). Anisotropic extinction effects resulting from crystal-shape anisotropy are taken into account by $\overline{T_\mu}$. Calculation of $\overline{T_\mu}$ was carried out with *Xtal* (Hall *et al.*, 1995). As a rule, $\overline{T_\mu}$ varies from one wavelength to another, and linear interpolations are given in Table 3.

The wavelength-dependent data were fitted to Zachariasen's expression using the Levenberg–Marquardt algorithm. The measurement uncertainties are composed of the counting statistical contribution and the uncertainty in the scale factors.

Table 3
Variation of the absorption-weighted mean path lengths in the range λ = 0.02–0.06 Å for the low-order reflections under investigation.

The interpolation is of the form $\overline{T_\mu}$ (mm) = $a - b\lambda$ (Å).

hkl	$\overline{T_\mu}$ (vanadium)	$\overline{T_\mu}$ (niobium)
110	2.478 − 0.115λ	2.549 − 0.386λ
101	2.357 − 0.450λ	2.437 − 2.646λ
01$\bar{1}$	2.326 − 0.314λ	2.483 − 2.714λ
200	2.333 − 0.499λ	2.448 − 2.765λ
020	2.357 − 0.451λ	2.481 − 2.697λ
002	2.501 − 0.082λ	2.435 − 2.231λ
211	2.335 − 0.462λ	2.405 − 1.301λ
121	2.360 − 0.675λ	
112	2.423 − 0.179λ	

Two parameters have been varied, the kinematical structure-factor amplitude $F(\lambda = 0)$ and the mosaic width parameter g. Graphs of data and fitting curves are displayed in Figs. 1 and 2, and the fit results have been included in Tables 1 and 2. It is seen that the wavelength dependence of extinction is adequately accounted for by Zachariasen's equation. The anisotropy in the fitted mosaic widths is about two: FWHM = 14.6 (3)–27.4 (6) arcsec for V, and FWHM = 1.63 (4)–3.77 (8) arcmin for Nb. The precision of the extrapolated squared structure factors is substantially better than 1%. Note that symmetry-equivalent reflections have not been constrained to satisfy equality for $F^2(\lambda = 0)$ but have been fitted independently. Nevertheless, the extrapolation leads to virtually identical kinematic structure factors, thus meeting a strict criterion for the assessment of the fits. In spite of the rather different mosaic widths, the amount of extinction is similar for the two crystals. The smallest extinction factors are $y_{\min} = 0.52$ for V and 0.65 for Nb. From consideration of the expression $x \sim gF^2$, which governs secondary extinction, it is seen that the effect of a decrease in g can be offset by an increase in F^2 arising from the higher electron number.

The practice of truncating the power-series expansion of the Zachariasen expression at the first-order term, $y \simeq 1 - x$, for linear extrapolation against λ^2 is only useful for very small x. When $x = 0.2$, one has $y = 0.845$, deviating more than 5% from the first-order approximation. In the present work, the largest values of x are 1.32 and 0.70 for V and Nb, respectively, and $y(\lambda)$ is evidently not a linear function of λ^2.

4. Discussion

It is instructive to make a comparison with other theoretical developments within the framework of the mosaic crystal model. The most popular extinction correction in crystallographic least-squares programs is that of Becker & Coppens (1974), where an additional term is introduced in the square-root function for y to take account of the angular dependence and severity of extinction. Angular-dependent extinction effects are negligible in γ-ray diffraction. Application of the Becker & Coppens expression for a Lorentzian mosaic distribution leads to the conclusion that it is just as successful as Zachariasen's expression. For Nb(200) and Nb(020), one obtains $F^2(\lambda = 0) = 2854$ (13) and 2851 (13), respectively, in close agreement with the values from Table 1. Use of a Gaussian distribution within the Becker & Coppens formalism leads to somewhat poorer fits. According to Ockham's razor, more complex models should not be preferred over simpler ones when both explain available data equally well. This maxim singles out Zachariasen's function. It is noteworthy that no shortcomings of Zachariasen's theory have been found in previous model comparisons based on wavelength-

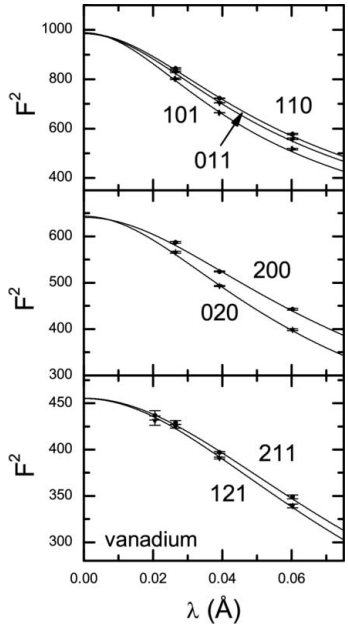

Figure 1
Observed squared structure factors on an absolute scale for vanadium. The solid lines are fits using Zachariasen's extinction function.

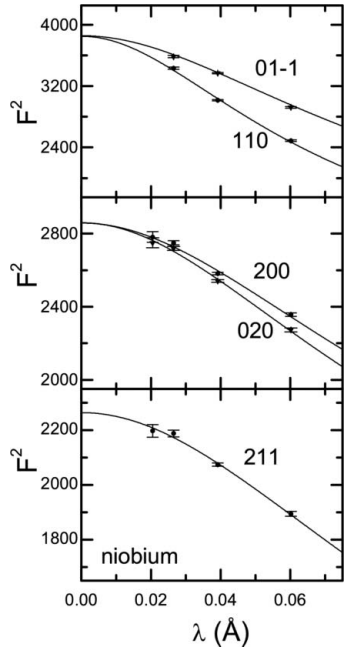

Figure 2
Observed squared structure factors on an absolute scale for niobium. The solid lines are fits using Zachariasen's extinction function.

dependent γ-ray and neutron time-of-flight data (Jauch *et al.*, 1988; Palmer & Jauch, 1995).

The Zachariasen and Becker & Coppens formalisms share the common assumption that there is no spatial correlation between the different mosaic blocks, so that in the limit of zero mosaic spread the crystal consists of parallel blocks separated by random displacements. According to Sabine's model (Sabine, 1992) of correlated blocks, a monolithic perfect crystal results for vanishing mosaic spread. Application of Sabine's expression for secondary extinction clearly demonstrates its inadequacy to describe the wavelength dependence. The χ^2 values are more than an order of magnitude larger than those for the Zachariasen model. The correlated block model is disproved by experiment (Palmer & Jauch, 1995).

It has been assumed so far that the crystals are subject to secondary extinction only. The expected magnitude of primary extinction deserves closer inspection. The primary extinction factor may be approximated by $y_p \simeq \exp[-(\delta/2)^2]$, where δ is the average size of the perfect domains in units of the extinction length $t_{\rm ext}$ [$= V/(\lambda F)$] (Suortti, 1982). The smallest value of $t_{\rm ext}$ is 34 µm for Nb(110) at $\lambda = 0.0602$ Å. Even if there were perfect regions as large as 5 µm in diameter, then primary extinction would be restricted to $y_p \geq 0.995$. Note that this limit refers to the worst case. The corresponding value for Mo $K\alpha$ radiation is $y_p \simeq 0.5$. The problematic coexistence of both types of extinction is thus avoided in γ-ray diffraction thereby allowing direct evaluation of pure secondary extinction.

It is of interest to compare the extrapolated values of F_o^2 with the calculated (extinction-free) values, F_c^2, as obtained from multipole model refinements of extended data sets. In the multipole model, the atomic electron density in a crystal is partitioned into core electron functions and a nucleus-centred expansion of spherical harmonic valence-density functions. For vanadium, symmetry-equivalent reflections from the set {211} were included in the multipole model refinement, the three extrapolated ones, and, concomitantly, eight equivalents measured at $\lambda = 0.0392$ Å ($y = 0.880$–0.887). For the three limit values one obtains, $R(F^2) = \sum |F_o^2 - F_c^2| / \sum F_o^2 = 0.0039$ and $R(\sigma) = \sum \sigma(F_o^2) / \sum F_o^2 = 0.0065$, whereas the eight extinction-affected reflections give $R(F^2) = 0.0070$ and $R(\sigma) = 0.0031$. For the extended complete data set, comprising 382 observations (102 of them unique), $R(F^2) = 0.0078$ and $R(\sigma) = 0.0057$. There is thus consistency between the data sets, with the limit values of the structure factors being in agreement with the predictions from the least-squares refinements. The agreement is less perfect in the case of Nb. A possible explanation is found in the lowered overdetermination concerning the adjustable valence-density parameters. Only a very few reflections carry information on the diffuse 4*d* valence shell, which are therefore most influential for their fitted counterparts.

Finally, it is worth considering whether kinematical conditions are within reach at synchrotron sources. For a given crystal, secondary extinction depends upon the product $\overline{T_\mu}\lambda^2$, other things being equal. It is apparent that a decrease in wavelength is much more efficient in its reduction than the use of a smaller specimen. For a diffraction experiment with 100 keV synchrotron X-rays from a 0.2 mm crystal, the amount of secondary extinction is the same as that found with 316.5 keV γ-rays and 2 mm samples, since both experiments share the same value of $\overline{T_\mu}\lambda^2$. This emphasizes that extinction-free X-ray structure factors from compounds containing heavier elements are generally unattainable by single-wavelength measurements.

5. Conclusion

In conclusion, it has been demonstrated that wavelength-dependent γ-ray diffraction can be used to resolve ambiguities in experimental structure-factor determination arising from anisotropic extinction. Zachariasen's theory provides a proper function that allows faithful extrapolation to the kinematical limit.

We would like to thank Dr H.-J. Bleif for valuable discussions.

References

Becker, P. J. & Coppens, P. (1974). *Acta Cryst.* A**30**, 129–147.
Hall, S. R., King, G. S. D. & Stewart, J. M. (1995). Editors. *Xtal3.4 Users Manual.* University of of Western Australia, Australia.
Hubell, J. H. & Seltzer, S. M. (1995). *National Institute of Standards and Technology Internal Report* 5632, http://www.physics.NIST.gov/PhysRefData/XrayMassCoef/cover.html.
Jauch, W. & Palmer, A. (2002). *Acta Cryst.* A**58**, 448–450.
Jauch, W. & Reehuis, M. (2009). *Phys. Rev. B*, **80**, 125126.
Jauch, W. & Reehuis, M. (2011). *Phys. Rev. B*, **83**, 115102.
Jauch, W., Schultz, A. J. & Schneider, J. R. (1988). *J. Appl. Cryst.* **21**, 975–979.
Lippmann, T. & Schneider, J. R. (2000). *J. Appl. Cryst.* **33**, 156–167.
Palmer, A. & Jauch, W. (1995). *Acta Cryst.* A**51**, 662–667.
Sabine, T. M. (1992). *International Tables for Crystallography*, Vol. C, pp. 530–533. Dordrecht: Kluwer.
Suortti, P. (1982). *Acta Cryst.* A**38**, 642–647.
Thornley, F. R. & Nelmes, R. J. (1974). *Acta Cryst.* A**30**, 748–757.
Zachariasen, W. H. (1967). *Acta Cryst.* **23**, 558–564.